



2016-17

DOI: <http://dx.doi.org/10.18535/ijsee/v4i10.01>**Photogeneration of Reactive Oxygen Species and Biological Activities of Two Quinones**

Authors

*Anitha R.<sup>1</sup>, Kalaimathi M.<sup>2</sup>, Southamani K.<sup>1</sup>, Sahayarani C.<sup>4</sup> and Yesu Thangam<sup>5</sup>*<sup>1,2,3,5</sup>PG & Research Center of Chemistry, Jayaraj Annapackiam College for Women (Autonomous), Periyakulam-625 601, affiliated to Mother Teresa Women's University Kodaikanal, Tamilnadu, India.<sup>4</sup>PG & Research Department of Zoology, Jayaraj Annapackiam College for Women (Autonomous), Periyakulam-625 601, affiliated to Mother Teresa Women's University Kodaikanal, Tamilnadu, India

Email: sryeu@gmail.com

Photogenerating efficiency of two naphthoquinones, 2-methyl-7-methoxy-3-chloromethyl-1,4-naphthoquinone (NQ1) and 7-methoxy-2,3-bis-(chloromethyl)-1,4-naphthoquinone (NQ2) is evaluated using *N,N*-dimethyl-4-nitrosoaniline (RNO) bleaching assay and electron magnetic resonance (EMR) study. The singlet oxygen generating efficiencies of the quinone are determined relative to rose Bengal (RB). Superoxide dismutase (SOD) inhibitable cytochrome *c* reduction assay is used to determine the superoxide anion radical ( $O_2^{\cdot-}$ ) yield upon photoirradiation. Cyclic voltammetry studies indicate a correlation between  $O_2^{\cdot-}$  generation efficiency and redox potential of quinones. In addition, antimicrobial activity of these quinones is also investigated. Photoinduced DNA scission studies show that reactive oxygen species (ROS) is involved in the DNA strand break.

**Key words:** Quinones, singlet oxygen, spin trapping, superoxide anion, DNA cleavage.

Quinones play a vital role in therapeutic activities and 1,4-quinones possess potent anti-tumor, antifungal and antibacterial activities [1]. A characteristic feature of the quinone moiety is its ability to undergo reversible oxidation-reduction and form semiquinone and the subsequent reactive oxygen species (ROS) and these ROS are responsible for most of the anticancer activity of quinones. Quinones extracted from *Dalbergia sissooides* are reported to have photodynamic action, antimicrobial activity and the ability to cleave DNA [2]. ROS is a collective term that includes oxygen radicals and also some non-radical derivatives of oxygen like hydrogen peroxide (H<sub>2</sub>O<sub>2</sub>), hypochlorous acid (HOCl), superoxide anion radical ( $O_2^{\cdot-}$ ) and singlet oxygen ( $^1O_2$ ) [3]. ROS generated during redox cycling of quinones results in the formation of DNA strand breaks [4]. The biological consequences of free radical formation by antitumor quinones are well known [5]. Administration of ROS generating compounds forms a useful strategy in the treatment of solid tumors [6]. In view of the biological activities of various quinones, in this work the photogeneration of ROS from NQ1 and NQ2 were evaluated. The antimicrobial activities and the DNA cleavage studies were also investigated.

The quinones, 2-methyl-7-methoxy-3-chloromethyl-1,4-naphthoquinone (NQ1) and 7-methoxy-2,3-bis-(chloromethyl)-1,4-naphthoquinone (NQ2), were used in this work and their structures are given below:

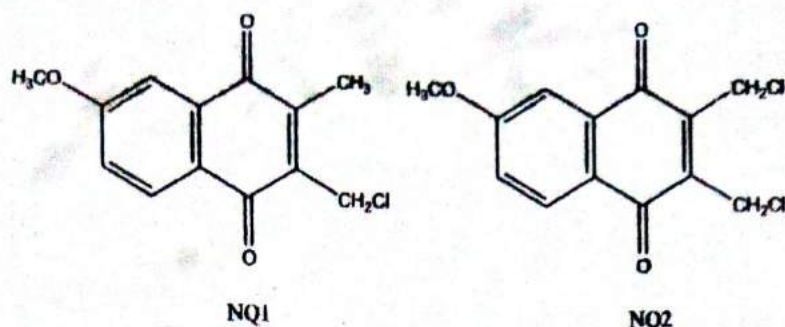


Fig.1. Chemical structures of 2-methyl-7-methoxy-3-chloromethyl-1,4-naphthoquinone (NQ1) and 7-methoxy-2,3-bis-(chloromethyl)-1,4 (NQ2).

Light source used for irradiation was a 150 W xenon lamp. A filter combination of 10-cm potassium iodide solution (1 g in 100 ml) and 1-cm pyridine was used to cut off below 300 nm and to achieve a spectral window of 300 - 700 nm. The reaction mixture in a quartz cuvette, was continuously stirred during irradiation. Optical measurements were made using Shimadzu UV-VIS spectrometer (UV-160). For EMR spectral measurements a JEOL JES-TE100 ESR spectrometer was used.

### 3.1. RNO bleaching assay

To investigate the generation of singlet oxygen, RNO bleaching assay was used [7]. The sensitizers, NQ1 and NQ2 were exposed to light in the presence of imidazole (10 mM) and RNO (50 mM) in phosphate buffer (pH = 7.4). The rate of disappearance of quencher (A) obeys the following equation:

$$\frac{d[A]}{dt} = \frac{(I_{ab}\Phi^1O_2)K_r[A]}{K_d}$$

where,  $K_r$  is the rate constant for chemical quenching of  $^1O_2$  by A,  $K_d$  is the rate constant for deactivation of  $^1O_2$  by solvent and  $I_{ab}$  is the intensity of light absorbed by the sensitizer. Each compound under investigation along with the reference singlet generator RB, was studied under identical conditions. The relative ratio of the slopes of the quinones and RB, after correction for molar absorption and photon energy [8] was used to compute the relative efficiency of singlet oxygen generation taking  $\Phi(^1O_2) = 0.76$  for RB [9]. To support the formation of  $^1O_2$ , the RNO bleaching experiment was followed in the presence of specific  $^1O_2$  quencher such as DABCO and sodium azide. The  $^1O_2$  quenching rate constants of imidazole ( $2 \times 10^7 \text{ M}^{-1} \text{ s}^{-1}$ ) and DABCO ( $1.5 \times 10^7 \text{ M}^{-1} \text{ s}^{-1}$ ) are comparable [10]. Hence when the photobleaching experiment was carried out in the presence of equimolar amounts of both these compounds, the observed rate would be decreased by about half.

### 3.2. EMR-TEMPL method

Photogeneration of  $^1O_2$  was further confirmed by EMR studies using 2,2,6,6-Tetramethyl piperidinol (TEMPL) as singlet oxygen probe [11]. Reaction mixture (1 ml) containing 0.01 M TEMPL and 0.2 mM quinone in DMSO was irradiated, inserted into a quartz tube and placed in the EMR cavity for measurements. The increase in EMR signal intensity of the 2,2,6,6-tetramethyl-4-piperidinol-N-oxyl (TEMPOL) radical produced was monitored.

### 3.3. SOD-inhibitable cytochrome c reduction assay

Superoxide anion radical was detected by the reduction of Fe(III)-Cyt.c by  $O_2^{\cdot -}$ . Solutions of quinones (100  $\mu\text{M}$ ) were photolysed in the presence of ferricytochrome c (40  $\mu\text{M}$ ) in 50 mM phosphate buffer (pH = 7.4). The generation of ferrocytochrome c was monitored spectrophotometrically at 550 nm using  $\Delta OD_{550} = 20000 \text{ M}^{-1} \text{ cm}^{-1}$  for reduced-oxidised cytochrome c [12]. Generation of superoxide anion radical from the quinones in the presence of EDTA was also followed optically.

### 3.4. EMR spin trapping method

This method was also used for the detection of  $O_2^{\cdot-}$ . [13]. The reaction mixture (1 ml), containing quinones (200  $\mu$ M) and DMPO (100 mM) in DMSO, placed in a quartz cuvette, and EMR was measured. Experiments were repeated to monitor the signal intensity at different intervals of irradiation time. The transient radical species were trapped by DMPO to form DMPO-adducts. The spectral identification was confirmed by computer simulation using a BASIC computer program. The output from this program was plotted to get the simulated spectra.

### 3.5. Cyclic voltammetry

Redox potentials of quinones (1 mg; 5 ml acetonitrile) were measured in a BAS 50A electrochemical analyzer (Bioanalytical systems, West Lafayette, IN) using glassy carbon working electrode, platinum auxiliary electrode and Ag/AgCl reference electrode. Glassy carbon electrode was resurfaced with alumina before use. Tetra-*n*-butylammonium perchlorate (TBAP, 50 mM) was used as the supporting electrolyte. Each solution was purged with nitrogen for 10 minutes prior to measurement, and the cyclic voltammograms were recorded under nitrogen atmosphere.

### 3.6. Antimicrobial activity: antifungal and antibacterial tests

Muller Hinton agar medium was used to find out the antibacterial activity of compounds against Gram-positive bacteria, *Bacillus subtilis*, and Gram-negative bacteria, *Escherichia coli*. Chloramphenicol was used control. All selected species are fastidious microorganisms, safe for experimentation. On the Muller Hinton agar plate 0.1 ml of logarithmic phase bacterial culture was inoculated. Well was prepared on Muller Hinton agar plate using cork borer. 10  $\mu$ l of each compound (10 mM) was placed in the corresponding well and the plates were incubated at 30 $^{\circ}$  C for 24 hours. After 24 hours, the plates were observed for antibacterial activity. The activity was measured in terms of zone of inhibition against bacteria (Gram-positive and Gram-negative) appearing around the well. The antifungal activity on yeast, *Saccharomyces cerevisiae*, was also studied for the quinones.

### 3.7. Photoinduced DNA cleavage by quinones

An in vitro assay for DNA strand breaks, induced by ROS, depends on the migration rates of supercoiled (unnicked), relaxed circular (nicked), linear and degraded plasmid DNA in agarose gel electrophoresis. Plasmid DNA (Genetix Biotech Asia Pvt. Ltd) (3  $\mu$ g) was used for these studies. The quinone solution in phosphate buffer (pH = 7.4) was irradiated for 10 minutes in gas-permeable Teflon capillary tube. After the irradiation was over, 20  $\mu$ l aliquot of the mixture was loaded into 0.7 % agarose gel (pH = 7.4) in tris-acetate EDTA (TAE) buffer containing 0.05  $\mu$ g/ml ethidium bromide. The electrophoresis was carried out for 2 h at 50 V. After electrophoresis, the gels were illuminated with UV light and photographed. The gel electrophoretic mobility of relaxed circle DNA (form II) in agarose is about half that of supercoiled DNA (form I).

### 4.1. Generation of singlet oxygen-RNO bleaching assay

The rate of photobleaching of RNO by the quinones and RB as a function of irradiation time is shown in Fig.2. The singlet oxygen yields thus evaluated are 0.27 and 0.23, for quinones NQ1 AND NQ2, respectively. To further support the role of singlet oxygen in bleaching of RNO, experiments were carried out in the presence of specific  $^1O_2$  inhibitors such as DABCO. Inhibition of RNO bleaching was studied in the presence of equimolar amounts of imidazole (10 mM) and DABCO (10 mM) and it is shown for the quinones in Fig. 3. The RNO bleaching rate constants of imidazole and DABCO are comparable [13]. Hence the reduction rate is decreased by about by 50%, when compared to the rate of RNO bleaching in the absence of DABCO. This confirms the generation of  $^1O_2$  during the photodynamic process.

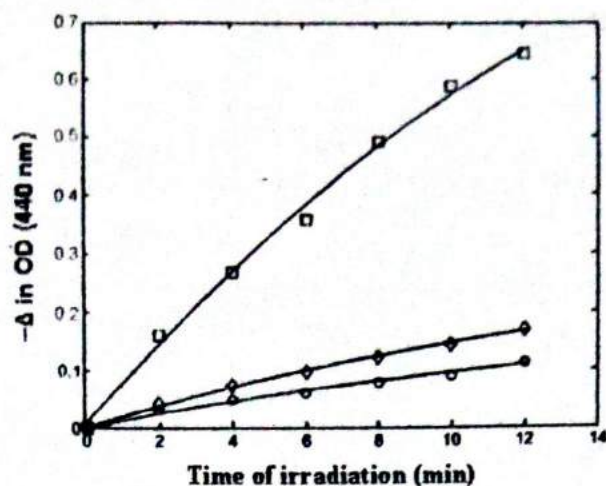


Fig. 2. Photosensitized RNO bleaching measured at 440 nm in the presence of imidazole (10 mM) in 50 mM phosphate buffer (pH = 7.4) with RB (□□□), NQ1 (◇◇◇) and NQ2 (○○○)

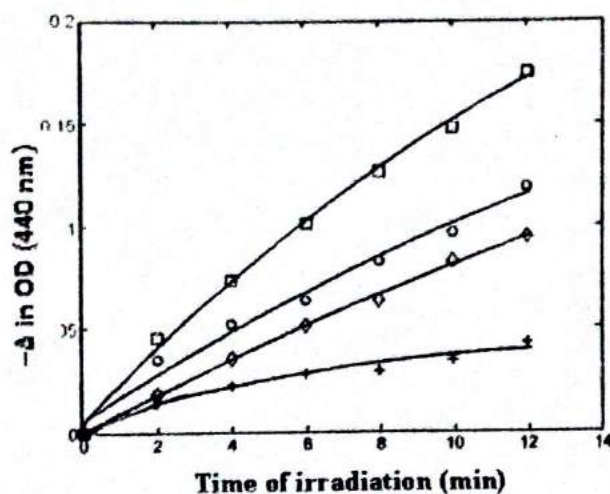


Fig. 3. Photosensitized RNO bleaching measure at 440 nm in the presence of imidazole (10 mM) in 50 mM phosphate buffer (pH = 7.4) with NQ1 (□□□) and NQ2 (○○○) as a function of irradiation time. Inhibition of photo-sensitized RNO bleaching by NQ1 (◇◇◇) and NQ2 (△△△) in the presence of 10 mM DABCO.

#### 4.2. EMR-TEMPL method

The generation of  $^1O_2$  was further confirmed by Electron magnetic resonance (EMR) method. The EMR spectrum of three equal intense lines, characteristic of TEMPOL nitroxide radical, was observed when aerated DMSO solutions of NQ1 and NQ2 were irradiated in the presence of TEMPL at room temperature. EMR signal intensity of photoproduced TEMPOL was found to increase with increase of irradiation time as shown in Fig. 4. RB also showed the formation of TEMPOL under the same conditions. The addition of sodium azide,  $^1O_2$  quencher, suppressed the EMR signal intensity of TEMPOL, confirming the formation of  $^1O_2$  (Fig. 4.)

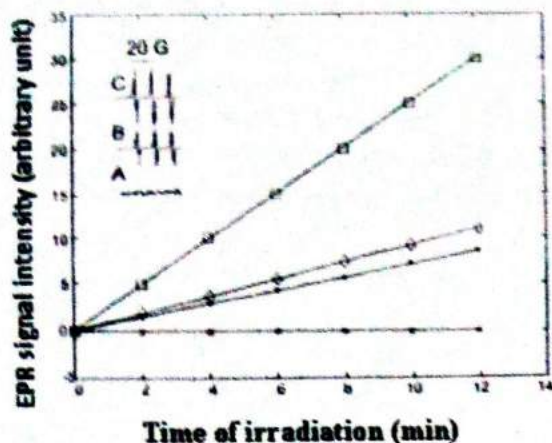


Fig. 4. The formation of TEMPOL during the photoillumination of solutions RB(TTT), NQ1 (◇◇◇) and NQ2 (\*\*\*) in the presence of TEMPL (20 mM) at 300 K in DMSO. Inhibitory effect of 2 mM sodium azide (\*\*\*) on the intensity of TEMPOL radical during photoirradiation of NQ1. (A) NQ1 in the dark; (B) 2 minutes irradiation and (C) 6 minutes irradiation.

#### ● Detection of superoxide anion radical

Fig. 5. shows the rate of cytochrome c reduction efficiencies of NQ1 and NQ2 when air saturated solution of the quinones were irradiated in the presence of cytochrome c (40  $\mu$ M) in phosphate buffer (50 mM) pH = 7.4. The rates of superoxide generation by NQ1 and NQ2 are found to be 0.037 and 0.026  $\mu$ M/s, respectively.

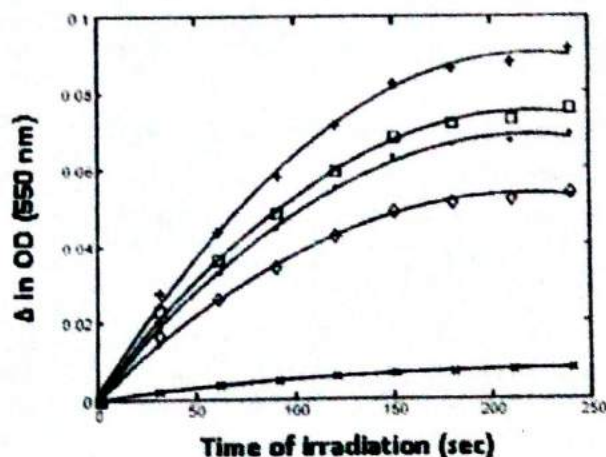


Fig. 5. Photosensitised superoxide generation measured as the rate of cytochrome c reduction in 50 mM phosphate buffer, pH = 7.4 by NQ1 (□□□), NQ1 + EDTA (+++), NQ2 (◇◇◇), NQ2 + EDTA (\*\*-), and NQ1 + SOD (xxx) as a function of irradiation time

The electron donor EDTA enhanced the rate of cytochrome c reduction when NQ1 and NQ2 were used as sensitizers and the rates were found to be 0.042 and 0.031  $\mu$ M/s (Fig. 5). Enhancement of photogeneration of  $O_2^{\cdot -}$  in the presence of electron donors is indicative of anionic properties of the radical intermediate formed during photosensitization [14]. Addition of SOD (50  $\mu$ g/ml) was found to inhibit the cytochrome c reduction.

#### 4.4. EMR spin trapping method

The generation of  $O_2^{\cdot -}$  was further confirmed by EMR spin trapping experiments with DMPO as the spin trap. EMR signal was not observed when DMPO or DMSO alone was irradiated. No EMR signal was

formed in the darkness from a sample containing the quinone (100  $\mu\text{M}$ ) and DMPO (100  $\mu\text{M}$ ) (Fig. 6A.). A multiline EMR spectra was obtained when NQ1 was photolysed in air-saturated DMSO solution (Fig. 6B). The EMR signal intensity was found to increase with increase of irradiation time. The EMR spectrum could be readily analyzed in terms of a mixture of two types of spin adducts, which can be simulated based on two EMR spin adducts, assigned as  $\text{DMPO-O}_2^{\cdot-}$  and  $\text{DMPO-OH}$  (Fig. 6C).

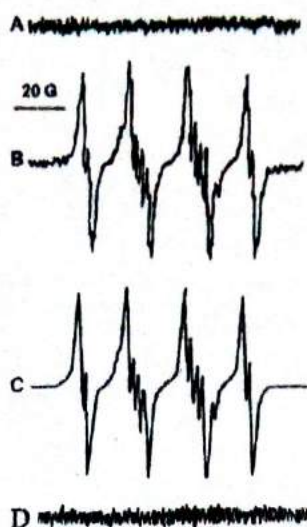


**Fig. 6** EMR spectrum obtained at room temperature in air-saturated DMSO solution by irradiation of NQ1 (100  $\mu\text{M}$ ) and DMPO (100  $\mu\text{M}$ ). (A) in the dark. (B) after 8 min irradiation. (C) computer-simulated spectrum, (D) in the presence of SOD (50  $\mu\text{g/ml}$ ). The spectrometer settings: microwave power, 2 mW; modulation frequency, 100 kHz; modulation amplitude, 0.5G; time constant, 0.1 sec.; scan rate, 4 min.; receiver gain, 500 and scan width 200 G.

Hyperfine coupling constant (hfcc) values for  $\text{DMPO-O}_2^{\cdot-}$  adduct were arrived to be  $A_N = 13.1$  G,  $A_H^{\beta} = 10.2$  G,  $A_H^{\alpha} = 1.41$  G and the other adduct was identified as  $\text{DMPO-OH}$  with the hfcc  $A_N = 14.9.0$  G,  $A_H = 14.7$  G. These hfcc are consistent with the reported values for  $\text{DMPO-O}_2^{\cdot-}$  and  $\text{DMPO-OH}$  adducts in DMSO [15]. Addition of SOD prior to irradiation of the quinones eliminated the EMR signal as shown in Fig. 6D, confirming the formation of  $\text{O}_2^{\cdot-}$ .

#### 4.5. Redox potential studies

To determine reduction potential of the quinones, NQ1 and NQ2 electrochemical studies were carried out. Cyclic voltammogram of NQ1 and NQ2 (Fig. 7) showed two cathodic peaks and two anodic peaks. The electrochemical data for NQ1 and NQ2 are given in Table 1. The observed reduction potential for NQ1 and NQ2 for wave one are  $-0.825$  and  $-0.632$  V, respectively. The quinone NQ1 has more reduction potential than NQ2. The half-wave potential of NQ1 is more negative than that of NQ2. Electron-donating substituents are known to cause a shift of  $E_{1/2}$  to more negative value [16].  $E_{1/2}$  values suggest NQ1 to be more readily reducible.

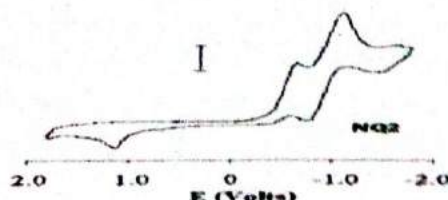


**Fig. 7.** Cyclic voltammograms of NQ2 in acetonitrile containing TBAP as supporting electrolyte (0.05M) at 100 mV/s scan rate.

**Table 1. Cyclic voltammetric data of NQ1 and NQ2**

Substrate	Wave I Peak Potential*				Wave II Peak Potential*			
	E <sub>pc</sub>	E <sub>pa</sub>	ΔE <sub>p</sub>	E <sub>1/2</sub>	E <sub>pc</sub>	E <sub>pa</sub>	ΔE <sub>p</sub>	E <sub>1/2</sub>
NQ1	-0.957	-0.694	0.263	-0.825	-0.185	-0.135	0.050	-0.160
NQ2	-0.714	-0.550	0.164	-0.632	-0.155	-0.067	0.088	-0.111

\*Potentials in V against Ag/AgCl; scan rate: 100 mV/s

#### 4.6. Biological activity

The *in vitro* antimicrobial activity of NQ1 and is given in Table 2. The zone of inhibition against Gram negative bacteria was found to be 0.14 and 0.19 for NQ1 and NQ2, respectively.

**Table 2. Antimicrobial activity of quinones NQ1 and NQ2**

S. No	Chemical compound	Zone of inhibition (Diameters in cm) against		
		Gram positive Bacteria*	Gram negative Bacteria <sup>†</sup>	Yeast cell <sup>‡</sup>
1	NQ1	-	0.14	0.09
2	NQ2	-	0.19	0.17

Bacillus subtilis; <sup>†</sup>Escherichia coli; Saccharomyces cerevisiae

1,4-Naphthoquinones with chlorine on the side chain are known to exhibit enhanced antibacterial activity via cell respiration inhibition than menadione against *Staphylococcus aureus* [17]. Among the halogenated 1,4-naphthoquinones, the chlorinated 1,4-naphthoquinones have increased antibacterial activity [18]. In the present study, quinone NQ2, which possess two chlorine substituents, showed more antibacterial activity than NQ1, in accordance with the earlier observations. No activity was found with Gram positive bacteria. Both NQ1 and NQ2 compounds showed antifungal activities against yeast, *Saccharomyces cerevisiae*, and their antifungal activity was found to be 0.09 and 0.17 cm in diameters for NQ1 and NQ2, respectively. Here again NQ2 has higher antifungal activity compared to NQ1.

#### 4.7. Photoinduced DNA cleavage

Quinone mediated photocleavage of covalently closed circular plasmid DNA was examined for NQ1 and NQ2 in phosphate buffer (pH = 7.4). Fig.8 shows the pictorial representation of the results obtained for the experiments for different concentrations of NQ1 and NQ2. Lane 1 contains DNA in dark and lane 2 has DNA with NQ1 (1 mM) in dark and these lanes serve as controls. Lanes 3 and 4 represent concentration-dependent photocleavage by NQ1. Lane 3 shows a decrease in the intensity of form I (supercoiled DNA) and a corresponding increase in the intensity of form II (relaxed DNA) for higher concentration of NQ1 (2 mM). Compared to lane 3, the intensity of form I is slightly higher in lane 4, and the intensity of form II is reduced for lower concentration of NQ1 (1 mM). Lanes 5 (1 mM) and 6 (2 mM) also show the effect of NQ2 on the DNA scission. In lane 5, compared to lane 1, shows decrease in the intensity of form I and increase in the intensity of form II. In lane 6, there is a slight increase in the intensity of form I and form II. Thus a concentration-dependent DNA scission is observed for NQ1 and NQ2 [19]. Comparison of lane 3 and 6 shows that NQ1 exhibits more photocleavage. These observations correlate well with the higher <sup>1</sup>O<sub>2</sub> and O<sub>2</sub><sup>-</sup> photogenerating efficiency of NQ1. Thus, in the *in vitro* photoactivated DNA scission, the role of ROS is well demonstrated. Results of cytochrome c reduction assay also show good correlation between O<sub>2</sub><sup>-</sup> generation and DNA scission. Any synthetic compound capable of cleaving DNA is considered to be a potential anticancer drug [20] and quinones NQ1 and NQ2 can be studied further for their therapeutic activity.

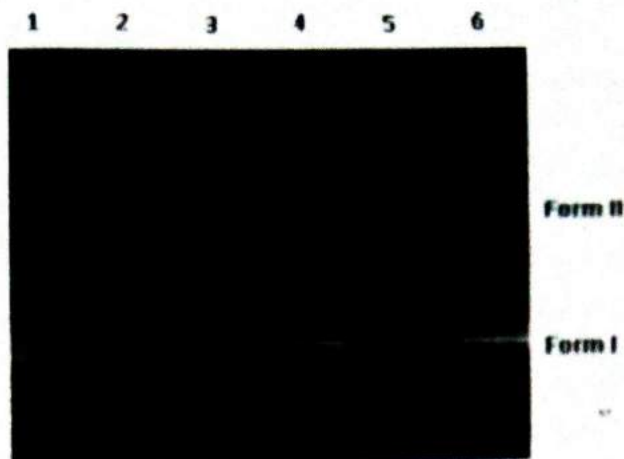


Fig. 8. Photoinduced scission of plasmid DNA (3  $\mu$ g) mediated by NQ1 and NQ2 in phosphate buffer (pH = 7.4). Lanes: 1) DNA alone in dark; 2) DNA + NQ1 in dark; 3) DNA + NQ1 (2 mM); 4) DNA + NQ1 (1 mM); 5) DNA + NQ2 (1 mM); 6) DNA + NQ2 (2 mM);

In conclusion, in this work two 1,4-quinones, viz., 2-methyl-7-methoxy-3-chloromethyl-1,4-naphthoquinone (NQ1) and 7-methoxy-2,3-bis-(chloromethyl)-1,4-naphthoquinone (NQ2), are investigated for their efficiency to photogenerate singlet oxygen ( $^1O_2$ ) and superoxide anion radical ( $O_2^{\cdot-}$ ). Yields of  $^1O_2$  upon photoirradiation, monitored by N,N-dimethyl-4-nitrosoaniline (RNO) bleaching assay, relative to rose bengal, NQ1 and NQ2 are found to be 0.27 and 0.23, respectively. The production of  $O_2^{\cdot-}$  radical is enhanced in the presence of electron donors such as EDTA. Irradiation of NQ1 and NQ2 photogenerate  $O_2^{\cdot-}$  and  $\cdot OH$  radicals as evidenced by EMR spin trapping using DMPO. NQ1 and NQ2 possess the ability to generate reactive oxygen species. The enzymatic ROS generation by quinones correlates with the redox potential. The observed photoinduced cleavage of DNA also lends evidence for the ROS generating efficiency of these quinones.

#### Acknowledgement

The authors are grateful to the UGC for providing the Major Research Grant to carry out this work at Jayaraj Annapackiam college (Autonomous) for Women, Periyakulam.

1. Lin A.J., Sartorelli A.C., Potential bioreductive alkylating agents-VI. *Determination of the relationship between oxidation-reduction potential and antineoplastic activity*, *Biochemical Pharmacology* 25, 206, 1976.
2. Yesu Thangam Y., Mothilal K.K., Gandhi dasan R., Murugesan R., "Photodynamic action and antimicrobial activity of some excited metabolites of *Dalbergia sissooides* and their ability to cleave DNA", *Natural Product Communications*, 2, 159-168, 2007.
3. Halliwell B., *Antioxidants and human disease: A general Introduction*, *Nutri. Rev.* 55, 544, 1997.
4. Gibson N.W., Hartley J.A., Butler J., Siegel D., Ross D., *Relationship between DT-diaphorase-mediated metabolism of a series of aziridinybenzoquinones and DNA damage and cytotoxicity*, *Mol. Pharm.* 42, 531, 1992.
5. Dichancaite E., Cenas N., Kalvelyte A., Sarapiniene N., *Toxicity of daunorubicin and naphthoquinones to HL-60 cells: an involvement of oxidative stress*, *Biochem. Mol. Biol. Int.* 41, 987, 1997.
6. Powis G., *Free radical formation by antitumor quinines*, *Free Radic. Biol. Med.* 6 63, 1989.
7. Barja G., Herrero A., *Oxidative damage to mitochondrial DNA is inversely related to maximum life span in the heart and brain of mammals*, *FASEB J.* 14, 312, 2000.
8. Kraljic L., El Mohsni S., *A new method for the detection of singlet oxygen in aqueous solutions*, *Photochem. Photobiol.* 28, 577, 1978.



9. Gandin E., and Lion Y., *A simple and convenient method of measuring the number of photons absorbed by a solution irradiated with polychromatic light*, J. Photochem. 20, 77-81, 1982.
10. Lee P.C.C., and Rodgers M.A.J., *Laser flash photokinetic studies of rose bengal sensitized photodynamic interactions of nucleotides and DNA*, Photochem. Photobiol. 45, 79-86, 1987.
11. Wilkinson F., Brummer J.G., *Rate constants for the decay and reactions of the lowest electronically excited singlet state of molecular oxygen in solution* J. Phy. Chem. Ref. Data 10, 809, 1981.
12. Moan J., and Wold E., *Detection of singlet oxygen production by ESR*, Nature 279 450-451, 1979.
13. Koppenol W.H. and Butler J., *The radiation chemistry of cytochrome c*, Isr. J. Chem. 24, 11-16, 1984.
14. Buettner G.R. and L.W. Oberley, *Considerations in the spin trapping of superoxide and hydroxyl radical in aqueous systems using 5,5-dimethyl-1-pyrroline-1-oxide*, Biochem. Biophys. Res. Commun. 83, 69-74, 1978.
15. Diwu Z. and Lown J.W., *Photosensitization with anticancer agent, EPR studies of photodynamic action of hypericin: Formation of semiquinone radical and activated oxygen species on illumination*, Free Radic. Biol. Med. 14, 209-215. 1993.
16. Ozawa T. and Hanaki A., *Hydroxyl radical produced by the reaction of superoxide ion with hydrogen peroxide: Electron spin resonance detection by spin trapping*, Chem. Pharm. Bull. 26, 2572-2575, 1978.
17. Dribergen R.J., Verboom W., Reinhoudt D.N., Lelieveld P., *Electrochemistry of potential bioreductive alkylating quinones: its use in the development of new aziridinylquinones*, Anticancer Research, 6, 605, 1986.
18. Hansch C., Leo A., Unger S.H., Kim K.H., Nikaitaini D., Lien E.J., *"Aromatic" substituent constants for structure-activity correlations*, J. Med. Chem. 16, 1207, 1973.
19. V. Ambrogi, D. Artini, Ivo De Carneri, S. Castellino, E. Dradi, W. Logemann, G. Meinardi, M. Di Somma, G. Tosolini, E. Veechi, *Studies on the antibacterial and antifungal properties of 1,4-naphthoquinones*, British J. of Pharmacology, 40, 871, 1970.
20. J. Stubbe, J.W. Kozarich, *Mechanisms of bleomycin-induced DNA degradation*, Chem. Rev. 87, 1107, 1987.